EXPLICIT ACCUMULATION MODEL FOR GRANULAR MATERIALS UNDER MULTIAXIAL CYCLIC LOADING

THEODOR TRIANTAFYLLIDIS
TORSTEN WICHTMANN
ANDRZEJ NIEMUNIS

Institute of Soil Mechanics and Foundation Engineering,
Ruhr-University Bochum, Germany

The prediction of cyclic-driven accumulation of stress or strain in granular materials is difficult due to a number of subtile effects in the soil structure. Also from the numerical point of view such prediction turns out to be troublesome because even small systematic errors of the general-purpose constitutive models are quickly accumulated. A remedy could be a so called explicit model that treats accumulation as a kind of creep process especially for engineering problems like compaction or liquefaction. However, for a good assessment of accumulation a detailed definition of strain amplitude is required. Consideration of the polarization and the openness of strain cycles on one hand and the degree of adaptation of the fabric on the other hand is crucial. A novel "back polarization" tensor is introduced to memorize the history of cyclic deformation. Multiaxial strain amplitude is defined considering the shape of the strain loop and rotation of principal directions of strain tensor. Some experimental evidence for the assumptions made is provided. Finally attempts to correlate the in-situ degree of adaptation with dynamic soil properties are reported.

1 Introduction

A considerable displacement of structures may be caused by an accumulation of the irreversible deformation of soil with load cycles. Even relatively small amplitudes may significantly contribute. This can endanger the long-term serviceability of structures which have large cyclic load contribution and small displacement tolerance (e.g. magnetic levitation train). Under undrained conditions similar phenomena may lead to an accumulation of pore water pressure, to soil liquefaction and eventually to a loss of overall stability.

From a physical point of view, displacements due to cyclic loading are rather difficult to describe. They depend strongly on several subtle properties of state (distribution of grain contact normals, arrangement of grains)

which cannot be expressed by the customary state variables (stress $\mathbf{T}$ and void ratio e) used in geotechnical engineering. From a numerical point of view, two computational strategies can be considered: an implicit and an explicit one (time integration is not meant here).

Explicit or *N-type* models are similar to creep laws in which in place of time the number of cycles N is used. Therefore rates are understood in terms of the number of cycles, i.e. $\dot{\sqcup} = \partial \sqcup / \partial N$. Generally, explicit models can be seen as special-purpose constitutive relations that are thought to predict the accumulation due to a bunch of cycles at a time. The recoverable (resilient) part of the deformation is calculated in a conventional way (using many strain increments per cycle) in order to estimate the amplitude. Having the amplitude we assume that it remains constant over a number of the following cycles. The permanent (residual) deformation due to packages of cycles is calculated with special empirical formulas, that can be deducted from laboratory tests. In 'semi-explicit' models the cyclic creep procedure is interrupted by so-called *control cycles* calculated incrementally. Such cycles are useful to check the admissibility of the stress state, the overall stability (which may be lost if large pore pressures are generated) and, if necessary, to modify the amplitude (it may change due to a stress redistribution).

Implicit constitutive models are general-purpose relations which reproduce each single load cycle by many small strain increments. The accumulation of stress or strain appears as a by-product of this calculation, resulting from the fact that the loops are not perfectly closed. Implicit strategies require much computation time and magnify systematic errors. This requires a constitutive model of unreachable perfection. These as well as some other numerical problems discussed by Niemunis (2000) speak for the application of an explicit strategy, especially if the number of cycles is large.

2 Material model

For an arbitrary state variable $\sqcup$ we define its average value $\sqcup^{\mathrm{av}}$ upon a cycle in such way that $\sqcup^{\mathrm{av}}$ is the center of the smallest sphere that encompasses all states $\sqcup^{(i)}$ of a given cycle. The average value $\sqcup^{\mathrm{av}}$ should not be mixed up with the *mean* value $\frac{1}{n}\sum_{i=1}^{n} \sqcup^{(i)}$. The amplitude is defined as $\sqcup^{\mathrm{ampl}} = \max \| \sqcup^{(i)} - \sqcup^{\mathrm{av}} \|$. A more elaborated definition of multiaxial amplitude is given further in this text.

Performing triaxial tests we use the Roscoe variables $p = -tr(\mathbf{T})/3$ and $q = \sqrt{3/2}\,\|\mathbf{T}^*\|$ and the conjugated strain rates D_v and D_q with the scalar product $p\ D_v + q\ D_q = -\mathbf{T} : \mathbf{D}$. $\mathbf{D}$ is the strain rate and $\sqcup^*$ denotes the deviatoric part of $\sqcup$. In the triaxial case strain and stress are axial-symmetric. We denote the axial components of stress (only effective stresses are considered) and strain with the index $\sqcup_1$ and the lateral components with $\sqcup_2$ and $\sqcup_3$ using the principal stresses $p = -(T_1 + 2T_3)/3$ and $q = -(T_1 - T_3)$ and the conjugated strain rates $D_v = -(D_1 + 2D_3)$ and $D_q = -2/3\ (D_1 - D_3)$. Stress ratio is expressed by $\eta = q/p$ or $\bar{Y} = (Y - 9)/(Y_c - 9)$ with $Y = -I_1 I_2/I_3$, $Y_c = (9 - \sin^2\varphi)/(1 - \sin^2\varphi)$ and I_i being the invariants of $\mathbf{T}$. In the cyclic triaxial tests presented below the vertical stress component was cyclically varied with an amplitude T_1^{ampl} at a constant average stress level $\mathbf{T}^{\mathrm{av}}$. Also $\zeta = T_1^{\mathrm{ampl}}/p^{\mathrm{av}}$ is used.

The strains under cyclic loading can be decomposed into a residual and a resilient part denoted by $\sqcup^{\mathrm{acc}}$ and $\sqcup^{\mathrm{ampl}}$, respectively. The accumulated strain $\varepsilon^{\mathrm{acc}} = \|\boldsymbol{\varepsilon}^{\mathrm{acc}}\| = \|\int \mathbf{D}^{\mathrm{acc}} \mathrm{d}N\|$ and its ratio $\omega = \varepsilon_v^{\mathrm{acc}}/\varepsilon_q^{\mathrm{acc}}$ are usually measured. The shear strain amplitude $\gamma^{\mathrm{ampl}} = (\varepsilon_1 - \varepsilon_3)^{\mathrm{ampl}} = \sqrt{3/2}\,\|(\boldsymbol{\varepsilon}^*)^{\mathrm{ampl}}\|$ is used in the evaluation of cyclic triaxial tests.

The general stress-strain relation has the form

$$\mathring{\mathbf{T}} = \mathsf{E} : (\mathbf{D} - \mathbf{D}^{\mathrm{acc}}) \tag{1}$$

wherein E denotes the elastic stiffness. The rate of strain accumulation $\mathbf{D}^{\mathrm{acc}}$ is proposed to be

$$\mathbf{D}^{\mathrm{acc}} = D^{\mathrm{acc}}\ \mathbf{m} = f_{\mathrm{ampl}}\ \dot{f}_N\ f_p\ f_Y\ f_e\ f_\pi\ \mathbf{m} \tag{2}$$

with the direction expressed by the unit tensor $\mathbf{m}$ (= flow rule) and with the intensity D^{acc} given by six partial functions f. For triaxial tests $\omega = \sqrt{\frac{3}{2}}\ \mathrm{tr}(\mathbf{m})/\|\mathbf{m}^*\|$ holds. The intensity of strain accumulation D^{acc} depends on the strain amplitude γ^{ampl} (function f_{ampl}), the number of cycles N (function $\dot{f}_N$), the average stress p^{av} (function f_p), $\bar{Y}^{\mathrm{av}}$ (function f_Y), the void ratio e (function f_e), the cyclic strain history $\boldsymbol{\pi}$ (function f_π) and the shape of the strain loop (via function f_{ampl}). The detailed forms of the functions are given in Sec. 3.

The first so-called *irregular* cycle generates, at least for fresh pluviated samples, a much larger residual deformation than the so-called *regular* (second and subsequent) cycles. In the explicit method the irregular and the first regular cycle are calculated implicitly (Fig. 1a). This is necessary for representative information about one full regular cycle to estimate the

strain amplitude, its polarization etc. The irregular cycle is not suitable for this purpose. Note that if the irregular cycle happened to be similar to the subsequent ones (to be actually regular) the above mentioned precaution in the finite element (FE) calculation is redundant but safe. Equation (2) describes only the accumulation during the regular cycles. Also all diagrams presented in Sec. 3 show the residual strain due to the regular cycles only.

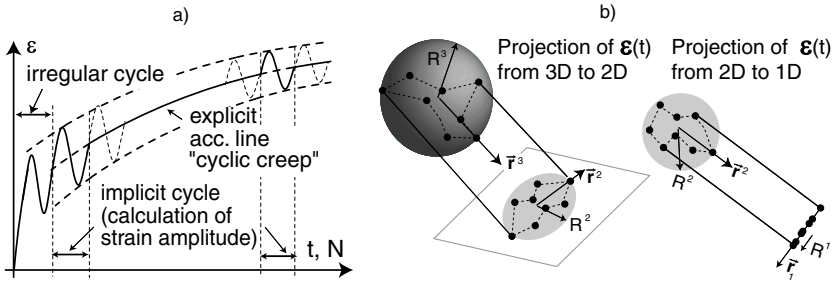

Figure 1 a) Calculation procedure in explicit models, b) Reduction steps (projections) from the 3-dimensional path to the 1-dimensional path

An important factor influencing $\mathbf{D}^{\mathrm{acc}}$ is the shape (openness) of the strain cycle. For example, a twirled multiaxial strain loop that encloses some volume in the strain space causes larger accumulation than a 1-D cycle of the same *scalar* amplitude. A more general definition of an amplitude is required, see also fatigue problem for metals, Ekberg (2000) and Papadopoulos (1994). In order to consider the openness and the complexity of the stress loop a novel definition is proposed here. The amplitude is assumed to be a fourth rank dyadic tensor. Experiments presented in Sec. 3 show that change in strain polarization increases the rate of accumulation. This effect is described in the following using a so-called "back polarization" tensor $\boldsymbol{\pi}$, which memorizes the cyclic strain history.

The multiaxial amplitude A_ϵ is defined as a combination of several specially chosen projections of the strain path (loop) weighted by their perimeters. Suppose that we are given a single strain loop in form of the strain path consisting of a sequence of discrete strain points $\boldsymbol{\epsilon}(t_i)$, $i = 1, \ldots, N$ (this loop need not be closed). These strain states lie in a 6-D strain space and need not be coaxial. The following flow chart demonstrates how to calculate the subsequent projections and their perimeters. The upper index indicate the number of dimensions of the strain space which need to be considered.

(1) Calculate the deviatoric projection $\mathbf{e}^5(t_i) = \boldsymbol{\epsilon}(t_i) - \frac{1}{3}\mathbf{1}\mathrm{tr}(\boldsymbol{\epsilon}(t_i))$ of the strain points $\boldsymbol{\epsilon}(t_i)$. For soils it was observed that only the deviatoric part of strain amplitude influences the process of cyclic relaxation or cyclic creep. The space in which the $\mathbf{e}^5(t_i)$-path could be drawn has 5 dimensions because the deviator of symmetric 3×3 tensor has 5 independent components.
(2) Calculate the perimeter $P_5 = \sum_{i=1}^{N} \|\mathbf{e}^5(t_i) - \mathbf{e}^5(t_{i-1})\|$ of the loop (define $\mathbf{e}^5(t_0) = \mathbf{e}^5(t_N)$ to close the loop) wherein N denotes the number of strain states (points) used to record the loop.
(3) Find the average point $\mathbf{e}^5_{\mathrm{av}}$ and the radius R_5 of the smallest 5-d sphere $R_5 = \|\mathbf{e}^5 - \mathbf{e}^5_{\mathrm{av}}\|$ that encompasses the loop (we may do it numerically using $\mathbf{e}_g = \frac{1}{N}\sum_{i=1}^{N} \mathbf{e}^5(t_i)$ as the first approximation of $\mathbf{e}^5_{\mathrm{av}}$).
(4) Calculate the unit tensor $\mathbf{r}^5$ along the line that connects the average strain $\mathbf{e}^5_{\mathrm{av}}$ with the most distant point $\mathbf{e}^5(t_i)$ of the loop. Usually there are two equally distant points (antipodes). In case of more than two equally distant points choose anyone of antipodes.
(5) Project the loop onto the plane perpendicular to $\mathbf{r}^5$ calculating $\mathbf{e}^4(t_i) = \mathbf{e}^5(t_i) - \mathbf{r}^5 : \mathbf{e}^5(t_i)\mathbf{r}^5$.
(6) Analogously find $P_4, R_4, \mathbf{r}^4$ and then $P_3, R_3, \mathbf{r}^3$, $P_2, R_2, \mathbf{r}^2$ and $P_1, R_1, \mathbf{r}^1$.

Reduction steps from the 3-D to the 1-D are shown in Fig. 1b. For any D-dimensional sub-space $\mathbf{e}^D$ is preserved in full tensorial (3×3) form. Doing this, the conventional definition of the distance, e.g. $R = \sqrt{[e_{ij} - e^{\mathrm{av}}_{ij}][e_{ij} - e^{\mathrm{av}}_{ij}]}$, remains insensible to the choice of the coordinate system.

After a series of projections a list of radii R_D, perimeters P_D and orientations $\mathbf{r}^D$ is calculated with dimensions $D = 1 \ldots 5$. The orientations are all mutually perpendicular, $\mathbf{r}^i : \mathbf{r}^j = \delta_{ij}$. The sense of the orientation $\mathbf{r}^D$ must not enter the definition of the amplitude. Therefore the dyadic products $\mathbf{r}^D\mathbf{r}^D$ are used and their weighted sum.

$$\mathsf{A}_\epsilon = \frac{1}{4}\sum_{D=1}^{5} P_D \; \mathbf{r}^D\mathbf{r}^D \tag{3}$$

is proposed to be the definition of the amplitude. The unit amplitude $\vec{\mathsf{A}}_\epsilon = \mathsf{A}_\epsilon / \|\mathsf{A}_\epsilon\|$ is further called *polarization*.

3 Experiments

The functions f_i in Eq. (2) are determined empirically on the basis of experimental data from cyclic triaxial and cyclic multiaxial direct simple shear (CMDSS) tests. The main experimental results are briefly summarized in the following. In all tests medium coarse sand (mean diameter $d_{50} = 0.5$ mm, uniformity index $U = d_{60}/d_{10} = 1.8$, maximum and minimum void ratios $e_{\max} = 0.874$, $e_{\min} = 0.577$) was used. The soil's density is described by $I_D = (e_{\max} - e)/(e_{\max} - e_{\min})$. The subscript $\sqcup_0$ denotes the initial value before cyclic loading.

3.1 *Cyclic triaxial tests*

Details of the cyclic triaxial apparatus, the specimen preparation procedure and the test results are given by Wichtmann *et al.* (2004a). Tests with varying amplitude, average stress and density were performed. All tests exhibit an increase of residual strain $\varepsilon^{\mathrm{acc}}$ with the number of cycles N with an accompanying decrease of the accumulation rate $\dot{\varepsilon}^{\mathrm{acc}}$.

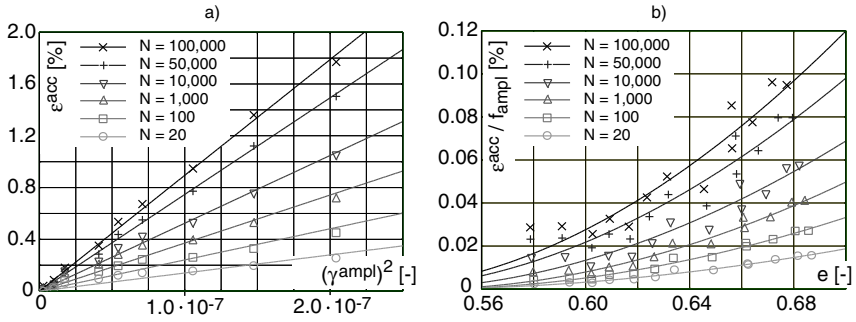

Figure 2 Rate of accumulation influenced by a) amplitude and b) void ratio

Tests with identical average stress $\mathbf{T}^{\mathrm{av}}$ ($p^{\mathrm{av}} = 200$ kPa, $\eta^{\mathrm{av}} = 0.75$) and similar initial density $I_{D0} = 0.55$–0.64 but different amplitudes T_1^{ampl} (10 kPa–90 kPa) exhibit a proportionality $\varepsilon^{\mathrm{acc}} \sim \left(\gamma^{\mathrm{ampl}}\right)^2$ independent on the number of applied cycles (Fig. 2a). Thus, f_{ampl} was proposed as

$$f_{\mathrm{ampl}} = \left(\gamma^{\mathrm{ampl}}/\gamma_{\mathrm{ref}}^{\mathrm{ampl}}\right)^2 \tag{4}$$

with a reference amplitude $\gamma_{\mathrm{ref}}^{\mathrm{ampl}} = 10^{-4}$.

In tests with different initial densities (I_{D0} = 0.63–0.99) but identical average and cyclic stress (p^{av} = 200 kPa, η^{av} = 0.75, ζ = 0.3) an increase of accumulation with void ratio e was observed (Fig. 2b). The partial function f_e is proposed to be

$$f_e = \frac{(C_e - e)^2}{1+e} \; \frac{1+e_{\mathrm{ref}}}{(C_e - e_{\mathrm{ref}})^2} \tag{5}$$

with the material constant C_e and the reference void ratio $e_{\mathrm{ref}} = e_{\max}$.

Tests with varying average stress $\mathbf{T}^{\mathrm{av}}$ (p^{av} = 50–300 kPa, η^{av} = 0.25–1.375) but identical amplitude ratio ζ = 0.3 and similar initial densities (I_{D0} = 0.57–0.69) show a faster accumulation with decreasing average mean pressure (Fig. 3a) and increasing stress anisotropy (Fig. 3b). For the purpose of purging the influence of slightly different shear strain amplitudes due to the dependence of sand stiffness on $\mathbf{T}$ the accumulated strain in Figs. 3a and 3b is divided by f_{ampl}. The exponential functions

$$f_p = \exp\left[-C_p \; \left(\frac{p^{\mathrm{av}}}{p_{\mathrm{ref}}} - 1\right)\right] \qquad f_Y = \exp\left(C_Y \; \bar{Y}^{\mathrm{av}}\right) \tag{6}$$

with C_p and C_Y being material constants and the reference pressure $p_{\mathrm{ref}} = p_{\mathrm{atm}}$ = 100 kPa were found to describe the experimental results .

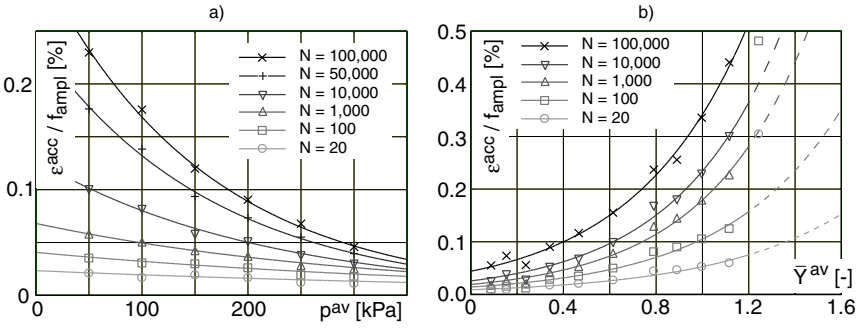

Figure 3 Rate of accumulation influenced by a) average mean pressure and b) stress anisotropy

Figure 4a presents the accumulated strain $\varepsilon^{\mathrm{acc}}$ in all test series adressed above divided by the partial functions f_p, f_Y, f_{ampl}, f_e and f_π (f_π = const = 1 in the cyclic triaxial case) as a function of the number of cycles. The curves in Fig. 4a exhibit an increase of accumulated strain faster than the logarithm of N. The current description of the dependence of the

accumulation rate on the number of cycles is

$$\dot{f}_N = C_{N1} \left[\frac{C_{N2}}{1 + C_{N2}\, N} + C_{N3} \right] \tag{7}$$

and drawn as the solid line in Fig. 4a. A more sophisticated model using a compaction tensor and passing on the function $\dot{f}_N$ is under way.

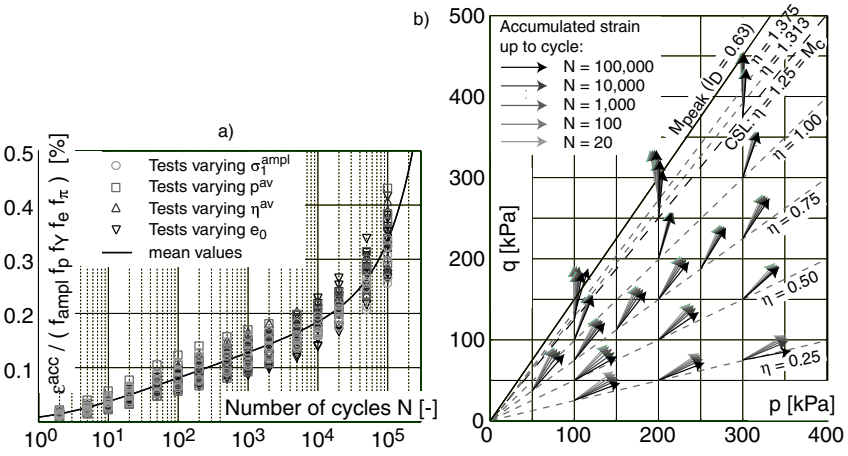

Figure 4 a) Rate of accumulation influenced by the number of cycles, b) flow rule

The flow rule $\mathbf{m}$ was found to be independent on density and amplitude but strongly dependent on $\mathbf{T}^{\mathrm{av}}$ as presented in Fig. 4b. In Fig. 4b the critical state line (CSL) is presented with an inclination $M_c = (6 \sin\varphi)/(3 - \sin\varphi) = 1.25$ in the p - q - space where $\varphi = 31.2°$ is the critical friction angle determined in static tests. At an average stress $\mathbf{T}^{\mathrm{av}}$ below the CSL cyclic loading leads to compaction whereas dilation is observed for $\eta^{\mathrm{av}} > M_c$. A slight increase of the volumetric portion of $\varepsilon^{\mathrm{acc}}$ with N was observed but currently this effect is not incorporated in our cyclic accumulation model. The well known flow rules of constitute models for monotonic loading (e.g. Cam-clay and hypoplastic models) are sufficient.

3.2 *Cyclic multiaxial direct simple shear (CMDSS) tests*

A special simple shear device was constructed to study the material behavior under cyclic multiaxial shearing. The apparatus allows to compare the accumulation under one-dimensional cyclic shear with the residual strain

due to an application of circular strain paths. Furthermore the influence of strain polarization of cyclic shear can be studied in this device since the direction of shear can be orthogonally changed after a given number of cycles. A detailed description of the apparatus, the procedure of specimen preparation and the test series is given by Wichtmann *et al.* (2004b).

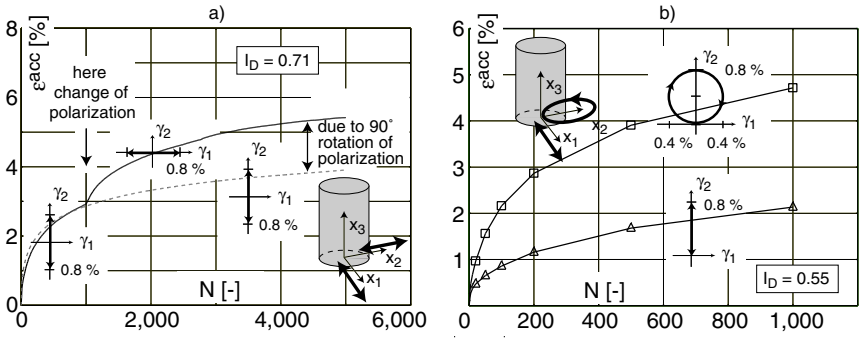

Figure 5 Rate of accumulation influenced by a) rapid change of strain polarization, b) shape of strain loop

Figure 5a presents the accumulation of strain measured in two tests with $\gamma^{\text{ampl}} = 8 \cdot 10^{-3}$. In the first test 5,000 cycles of one-directional cyclic shear were applied whereas in the second test the direction of shear was changed for 90° after 1,000 cycles and 4,000 cycles in the new direction followed. From Fig. 5a it is obvious that the change of strain polarization leads to a significant increase in accumulation rate. In order to mathematically describe these experimental findings the partial function f_π and the evolution of $\boldsymbol{\pi}$, respectively were proposed as

$$f_\pi = 1 + C_{\pi 1}\left[1 - \left(\vec{\mathbf{A}}_\epsilon :: \boldsymbol{\pi}\right)^{C_{\pi 2}}\right] \qquad \mathring{\boldsymbol{\pi}} = C_{\pi 3}\left(\vec{\mathbf{A}}_\epsilon - \boldsymbol{\pi}\right) \|\mathbf{A}_\epsilon\|^2 \qquad (8)$$

with $C_{\pi 1}, C_{\pi 2}$ and $C_{\pi 3}$ being material constants. Figure 5b contains a comparison of strain paths with circular and one-directional cyclic shear having identical amplitudes $\gamma^{\text{ampl}} = 8 \cdot 10^{-3}$ in one direction. The circular strain path leads to a twice larger accumulation in comparison with the one-directional cyclic shearing. This effect is captured by the definition of the amplitude $\mathbf{A}_\epsilon$.

4 Problem with N_0

Experimental observations indicate a strong dependence of the accumulation rate on the preloading history. Despite identical void ratios and stresses the accumulation rates $\dot{e}$ of two specimens may be quite different depending on their cyclic preloading history. A volume of sand *in situ* is less compactable than a freshly pluviated laboratory specimen. The preloading history (i.e. the number of cycles, the amplitudes and the polarization of the cycles) has to be determined. For the present the cyclic history is lumped together into a single scalar variable N_0 that enters the equation for $\dot{f}_N$ as the *initial number of cycles*.

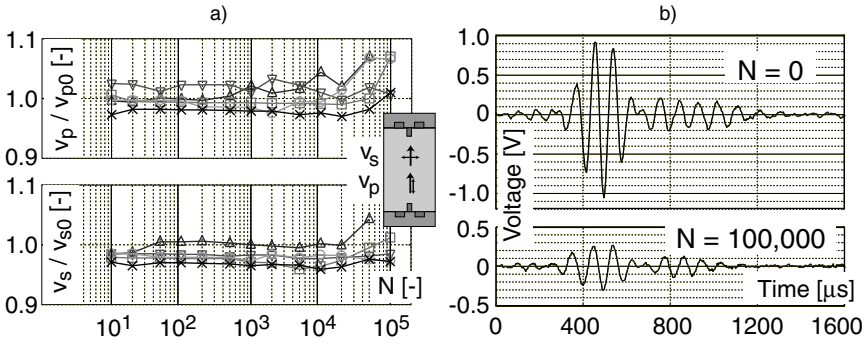

Figure 6 Impact of preloading history on a) v_p and v_s and b) signal intensity

Cyclic triaxial tests were performed in a test apparatus instrumented with piezoelectric elements for measuring compression (v_p) and shear (v_s) wave velocities. Details of the apparatus and the test series can be found in Wichtmann and Triantafyllidis (2004b). The cyclic loading was interrupted after given cycle numbers and v_p and v_s were measured at $\mathbf{T}^{\mathrm{av}}$. The development of the wave velocities with the number of cycles is presented in Fig. 6b for tests with varying average stress (p^{av} = 100–200 kPa, q^{av} = 100–200 kPa) but identical amplitude T_1^{ampl} = 60 kPa and similar initial densities (I_{D0} = 0.57–0.59). No significant changes of v_p and v_s and thus small strain stiffness could be detected. However, in the case of the elements that send and receive shear waves the intensity of the received signal tended to abate with the number of cycles, probably caused by an increased material damping. Further tests will check if N_0 can be correlated with damping.

Several undrained cyclic triaxial tests with drained preloading history exhibit a correlation between cyclic undrained strength (i.e. the stress amplitude T_1^{ampl} needed to cause a definite strain amplitude $\varepsilon_1^{\text{ampl}}$ in a given number of cycles) and N_0.

As an alternative for the determination of preloading history via indirect measurements N_0 could be detected by a back analysis of settlements caused by a strong vibration *in situ* (e.g. applied by a vibrator placed on the ground surface with accompanying measurements of the time history of nearby settlements).

5 Finite element (FE) calculation

The cyclic accumulation model was used to calculate a model test which was performed in the geotechnical centrifuge at our institute (Helm *et al.* 2000). In the model test (acceleration level 20g) a strip foundation (width 1 m) on a fine sand was loaded with an oscillating stress 104 kPa ± 69 kPa. After 70,000 cycles a settlement of 6.8 cm was observed below the middle of the foundation. The accumulation model predicts a settlement of 7.8 cm after 70,000 cycles (Fig. 7, Hammami 2003), which satisfactory agrees with the observations of the model test.

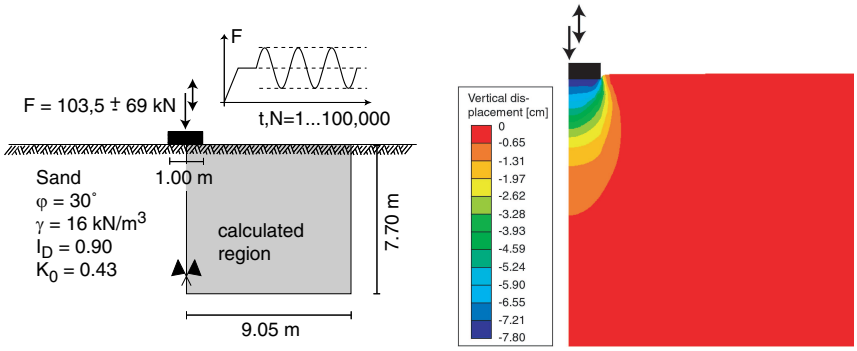

Figure 7 FE calculation of the settlement of a strip foundation under cyclic loading

Acknowledgements

The authors are grateful to German Research Council (DFG, Project A8 / SFB 398) for the financial support.

References

Ekberg, A. (2000). Rolling contact fatigue of railway wheels, Ph.D. thesis, Chalmers University of Technology, Solid Mechanics

Hammami, M. (2003). Numerische Fehler bei der expliziten FE-Berechnung der Verdichtbarkeit von Sand infolge zyklischer Belastung, Diploma thesis at Institute of Soil Mechanics and Foundation Engineering, Ruhr-University Bochum.

Helm, J., Laue, J. and Triantafyllidis, T. (2000). Untersuchungen an der RUB zur Verformungsentwicklung von Böden unter zyklischen Beanspruchungen, *Beiträge zum Workshop "Boden unter fast zyklischer Belastung: Erfahrungen und Forschungsergebnisse"*, Rep. No. 32, pp. 201–222.

Papadopoulos, I. (1994). A new criterion of fatigue strength for out-of-phase bending and torsion of hard metals. *International Journal of Fatigue*, **16**, pp. 377–384.

Niemunis, A. (2000). Akkumulation der Verformung infolge zyklischer Belastung - numerische Strategien, *Beiträge zum Workshop "Boden unter fast zyklischer Belastung: Erfahrungen und Forschungsergebnisse"*, Rep. No. 32, pp. 1–20.

Niemunis, A. (2003). Extended hypoplastic models for soils, *Habilitation*, Rep. No. 34, Institute of Soil Mechanics and Foundation Engineering, Ruhr-University Bochum.

Wichtmann, T. and Triantafyllidis, T. (2004a). Influence of a cyclic and dynamic loading history on dynamic properties of dry sand, part I: cyclic and dynamic torsional prestraining, *Soil Dynamics and Earthquake Engineering*, **24**, pp. 127–147.

Wichtmann, T. and Triantafyllidis, T. (2004b). Influence of a cyclic and dynamic loading history on dynamic properties of dry sand, part II: cyclic axial preloading, *Soil Dynamics and Earthquake Engineering (accepted)*.

Wichtmann, T., Niemunis, A. and Triantafyllidis, T. (2004a): Strain accumulation in sand due to drained uniaxial cyclic loading. *Cyclic Behaviour of Soils and Liquefaction Phenomena*, Proc. of CBS04, Bochum, March/April 2004, Balkema, pp. 233–246.

Wichtmann, T., Niemunis, A. and Triantafyllidis, T. (2004b): The effect of volumetric and out-of-phase cyclic loading on strain accumulation. *Cyclic Behaviour of Soils and Liquefaction Phenomena*, Proc. of CBS04, Bochum, March/April 2004, Balkema, pp. 247–256.